Meiosis arrest female 1 (MARF1) has nuage-like function in mammalian oocytes

You-Qiang Su[a,b], Fengyun Sun[a], Mary Ann Handel[a], John C. Schimenti[c], and John J. Eppig[a,1]

[a]The Jackson Laboratory, Bar Harbor, ME 04609; [b]State Key Laboratory of Reproductive Medicine, Nanjing Medical University, Nanjing 210029, People's Republic of China; and [c]College of Veterinary Medicine, Cornell University, Ithaca, NY 14853

This contribution is part of the special series of Inaugural Articles by members of the National Academy of Sciences elected in 2011.

Contributed by John J. Eppig, October 1, 2012 (sent for review August 4, 2012)

Orderly regulation of meiosis and protection of germline genomic integrity from transposable elements are essential for male and female gamete development. In the male germline, these processes are ensured by proteins associated with cytoplasmic nuage, but morphologically similar germ granules or nuage have not been identified in mammalian female germ cells. Indeed, many mutations affecting nuage-associated proteins such as PIWI and tudor domain containing proteins 5 and 7 (TDRD5/7) can result in failure of meiosis, up-regulation of retrotransposons, and infertility only in males and not in females. We recently identified MARF1 (meiosis arrest female 1) as a protein essential for controlling meiosis and retrotransposon surveillance in oocytes; and in contrast to PIWI-pathway mutations, *Marf1* mutant females are infertile, whereas mutant males are fertile. Here we put forward the hypothesis that MARF1 in mouse oocytes is a functional counterpart of the nuage-associated components of spermatocytes. We describe the developmental pattern of *Marf1* expression and its roles in retrotransposon silencing and protection from DNA double-strand breaks. Analysis of MARF1 protein domains compared with PIWI and TDRD5/7 revealed that these functional similarities are reflected in remarkable structural analogies. Thus, functions that in the male germline require protein interactions and cooperative scaffolding are combined in MARF1, allowing a single molecule to execute crucial activities of meiotic regulation and protection of germline genomic integrity.

Gamete development encompasses key cellular and molecular processes common to gametes of both sexes as well as sex-specific processes crucial for fertilization and embryogenesis. Common gametogenic pathways include meiosis, to carry out recombination and segregation of homologous chromosomes, and silencing of retrotransposons, to maintain genomic integrity. Precise control of these processes is essential for transmission of parental genetic materials to subsequent generations and creation of genetic diversity. Errors can cause infertility, miscarriage, or birth defects and pose genetic threats to the offspring and subsequent generations. Here we put forward the hypothesis that meiosis arrest female 1 (MARF1) expressed in mouse oocytes is a functional counterpart of the nuage-associated components of spermatocytes that carry out these crucial facets of regulation of meiosis and control of retrotransposon expression.

MARF1 Controls Meiosis and Retrotransposon Silencing in Female but Not Male Germ Cells in Mice

We previously used a forward genetics approach to identify genes controlling oogenesis and female fertility in mice, revealing a gene encoding a master regulator of oogenic processes (1). This gene, originally referred to as *4921513D23Rik*, is now named meiosis arrest female 1 (*Marf1*). Mutations of *Marf1* cause infertility only in females, a phenotype attributed to failure in oocyte maturation to progress beyond the germinal vesicle (GV)-stage and ovulation of immature GV stage oocytes. Up-regulation of protein phosphatase 2 catalytic subunit (PPP2CB) is a key feature of the meiotic arrest phenotype of *Marf1* mutant oocytes. This overexpression in *Marf1* mutant oocytes results in the failure to activate a maturation promoting factor that is essential for driving meiosis beyond prophase I (Fig. S1 shows a diagram illustrating the normal meiotic function of MARF1). Further studies on the mechanisms defining this phenotype led to uncovering significant defects in oogenic processes in *Marf1* mutant oocytes, including up-regulation of *Line1* and *Iap* retrotransposon mRNAs, which correlates with an increase in the number of nuclear DNA double-strand breaks. A cohort of other transcripts is also significantly up-regulated in the *Marf1* mutant oocytes, whereas very few transcripts are down-regulated, suggesting that the *Marf1* mutant phenotype results from aberrant RNA homeostasis and the absence of normal putative MARF1 RNase activity encoded by the NYN domain (Fig. 1). Thus, MARF1 controls meiosis and retrotransposon silencing in mammalian oocytes. Moreover, other oocyte developmental processes essential for preparation for fertilization and embryogenesis are also affected by *Marf1* mutation (1). A common thread uniting these seemingly disconnected oogenic processes is the disruption of oocyte RNA homeostatic mechanisms. Such homeostatic functions are not limited to MARF1 in oocytes but are complemented by the activities of endogenous small interfering RNAs (endo-siRNAs) (2, 3) as discussed later in more detail.

In contrast to females, male *Marf1* mutants are fully fertile, indicating apparently normal spermatogenesis. Thus, MARF1 function is required only during oogenesis. However, key gametogenic pathways, such as those controlling meiosis and suppression of retrotransposon expression, have counterparts in both the female and male germline, and in the context of sexually dimorphic mechanisms of gametogenesis it is instructive to examine both similarities and differences.

PIWI-Interacting (pi)RNA Pathway Controls Meiosis and Retrotransposon Silencing in Male but Not Female Germ Cells in Mice

The functions of MARF1 in female germ cells are reminiscent of a mechanism regulating meiosis and retrotransposon silencing in male germ cells. These functions involve the PIWI subfamily of the argonaute proteins and their interacting partners, such as certain members of the tudor domain-containing protein (TDRD) family and PIWI-interacting RNAs, known as piRNAs (4–6). These proteins and RNAs are localized to nuage or germ granules, which are germ cell-unique nonmembranous cytoplasmic microstructures aggregated with electron-dense ribonucleoprotein complexes (7, 8). Central to the control of spermatogenic processes by nuage components are the biogenesis of piRNA (9–11), piRNA-guided posttranscriptional cleavage of specific transposon

Author contributions: Y.-Q.S., M.A.H., J.C.S., and J.J.E. designed research; Y.-Q.S. and F.S. performed research; Y.-Q.S. and F.S. analyzed data; and Y.-Q.S., M.A.H., J.C.S., and J.J.E. wrote the paper.

The authors declare no conflict of interest.

[1]To whom correspondence should be addressed. E-mail: john.eppig@jax.org.

This article contains supporting information online at www.pnas.org/lookup/suppl/doi:10.1073/pnas.1216904109/-/DCSupplemental.

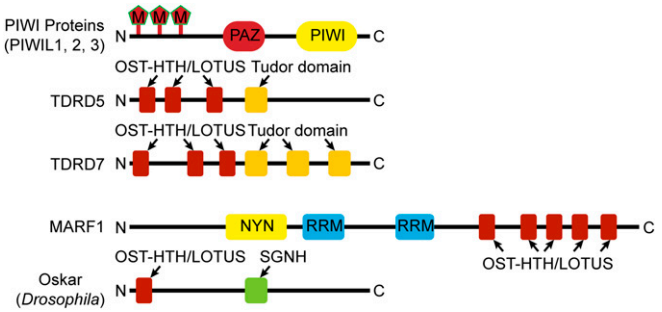

Fig. 1. Schematic representations of the composition of major domains in mouse PIWI proteins, TDRD5, TDRD7, and MARF1, and *Drosophila* Oskar proteins.

RNA by PIWI proteins (12), and piRNA-PIWI directed transcriptional suppression of transposon expression (12–14).

The piRNAs, generally 26–31 nucleotides in length, are a class of small noncoding RNAs processed from long single-stranded precursors in a DICER-independent mechanism. A significant number of piRNAs are derived from repetitive sequences, including retrotransposons, and are enriched in germline cells (11, 15–18). PIWI proteins are key components of nuage and play a central role in silencing transposable elements in germ cells (14, 19, 20). PIWI proteins have two major domains: the C-terminal PIWI domain and a central PAZ domain (Fig. 1) (21, 22). The RNase H-like endonuclease (slicer) activity of the PIWI domain is central to the function of some PIWI proteins and requires the binding of PIWI Argonaut and Zwille (PAZ) domains to piRNAs (23–25). The piRNAs bound by PAZ domains function as a guide for PIWI proteins by base-pairing to the cRNA targets (26). The function of PIWI proteins also requires interaction and coordination of PIWI proteins with other proteins, also residing in nuage. The partners most critical for the function of PIWI proteins are TDRDs, which are enriched in germ cell nuage (5, 27). The TDRDs contain various numbers of Tudor domains, which bind to symmetrically dimethylated arginines residues located in the N termini of PIWI proteins in specific combinations (28–31), thus functioning as scaffolds for multiple adaptors to recruit specific sets of interacting partners and targets to nuage (5, 27). PIWI proteins, facilitated by TDRDs and other interacting partners, catalyze the production of piRNAs from retrotransposon transcripts via their "slicer" activity, and thereby reduce the levels of retrotransposons at posttranscriptional levels (24, 25). PIWI proteins and piRNAs also silence retrotransposons at transcriptional levels by recruiting DNA methylation machinery to the retrotransposon promoter regions, facilitating methylation of CpG dinucleotides in this region (32, 33). Mutations in PIWI-coding genes cause defects in germ cell development, including the failure of germline stem cell maintenance and germ cell specification in both sexes of *Drosophila*, and meiotic arrest in *Drosophila* and mouse male germ cells, respectively, which culminates in infertility (19, 34–37).

Despite the well conserved existence of PIWI proteins, piRNAs, and other interacting partners of PIWIs in the germline of several animal species, the function of these proteins and piRNAs in mammals seems to be sex-biased and male-specific. In *Drosophila* and zebrafish, interruption of the PIWI-piRNA pathway affects both male and female fertility. In contrast, mutation of mouse genes encoding PIWI proteins (i.e., PIWIL1/MIWI, PIWIL2/MILI, and PIWIL4/MIWI2) and their direct and indirect interacting partners localized within nuage, such as TDRD1, TDRD5, TDRD7, TDRD9, MAEL, DDX4 (MVH), ASZ1 (GASZ), PLD6 (MitoPLD), and MOV10L1, all produce infertility only in males, but not females. The underlying causes are interruption of normal meiosis or spermiogenesis and up-regulation of the mRNAs encoding retrotransposons *Line1* and/or *Iap* (9, 10, 19, 36–46). The male-specific infertility phenotypes exhibited by these mutants suggests that the PIWI-piRNA pathway is not necessary for the control of meiosis and retrotransposon silencing in mammalian oocytes.

This unique facet of the sexual dimorphism in the control of mammalian meiosis may be attributable to the difference in the timing of genome-wide DNA methylation in mammalian germ cells. Meiosis in mammals is indeed sexually dimorphic, both in terms of the biological processes and the genetic control mechanisms (47, 48). Meiosis in female mammals initiates soon after sex determination in fetal gonads, whereas it does not commence in males until puberty. Unlike the continuous process of meiosis in males, meiosis in females is subjected to regulated starts and stops, with meiosis arrested at diplotene stage of the first meiotic prophase shortly after birth and throughout follicular development. Meiosis resumes in oocytes of nonatretic Graafian follicles only after a preovulatory surge of luteinizing hormone and is arrested again at metaphase II until fertilization. Mice bearing mutations in genes encoding several regulators of the earlier meiotic events often exhibit differences in the control of prophase I events in males and females (48–51). Interestingly, the timing of crucial reprogramming of DNA methylation also differs between males and females. De novo DNA methylation takes place in both female and male germ cells after genome-wide DNA demethylation in primordial germ cells, which allows reestablishment of the maternal and paternal specific imprints (52). The demethylation starts at approximately embryonic day (E) 7.5 when primordial germ cells (PGCs) migrate to and colonize at the genital ridge and is completed by E13.5 (53, 54). The genome-wide DNA remethylation takes place in males in prospermatogonia before birth, at approximately E13.5 and is completed 3 d after birth [postnatal day (P) 3] (55, 56). However, in females, DNA remethylation does not begin until after birth in growing oocytes that have already completed the earlier meiotic events and have progressed to the diplotene stage of prophase I (57). Thus, in males, remethylation is earlier in the development of the germline and premeiotic, whereas in females it is later in the development of the germline and postmeiotic prophase. Moreover, no prominent nuage or germ granules, similar to the intermitochondrial cement or chromatoid bodies present in male mouse germ cells, have been found in mouse oocytes (7). Although Balbiani bodies consisting of endoplasmic reticulum and mitochondria interspersed with nuage surrounding Golgi stacks have been reported in nongrowing mouse oocytes, they disappear soon after the oocytes commence their extensive growth phase (58). However, the global DNA demethylation reprogramming in primordial germ cells creates a window of vulnerability to possible escape and activation of transposable elements in both male and female germ cells. In the face of demethylation, mammalian germ cells of both sexes require mechanisms that defend against activation of retrotransposons. Thus, do female germ cells use mechanisms similar to the PIWI-piRNA pathway in male germ cells, or are there completely different female-specific mechanisms that control meiosis and retrotransposon silencing in mammalian oocytes?

Structural and Functional Analogies Between Oocyte MARF1 and Spermatocyte PIWI-piRNA Pathway

To address this question, we first asked whether there are any protein structure or molecular function similarities between MARF1 and the components of mouse male germ cell nuage involved in the PIWI-piRNA pathway.

The MARF1 protein has three major domain motifs: an N-terminal "LK-Nuc" domain, two central "RRM" domains, and C-terminal "OST-HTH/LOTUS" domains (Fig. 1) (59, 60). The "LK-Nuc" domain is now officially termed "NYN" (Nedd4-BP1, YacP Nucleases, NYN) domain, because of its original identification in the eukaryotic proteins Nedd4-binding protein 1 and the

bacterial YacP-like proteins. It is described as an RNase domain belonging to the superfamily that includes the 5′→3′ nuclease, PIN, NYN, and phage T4-type viral RNase H domains (61). The OST-HTH/LOTUS domain is a recently identified unique RNA-binding domain, which has a winged helix-turn-helix fold and is predicted to bind specifically to dsRNAs or stems of folded structures in RNAs (59, 60). This domain is also present in *Drosophila* Oskar and mammalian TDRD5/7 proteins (Fig. 1). Oskar is essential for the assembly of germ plasm in *Drosophila*, whereas TDRD5/7 proteins are required for formation of normal chromatoid bodies in mouse spermatids (39, 40, 62). Mutations in these genes cause failure of germ cell specification in *Drosophila* and interruption of normal spermatogenesis and retrotransposon repression in mice, respectively (39, 40, 63). Because dsRNAs formed by micro(mi)RNAs, repeat associated siRNAs, and piRNAs hybridized to their targets are readily found in nuage, Oskar and TDRD5/7 could potentially perform their function as "adapters" by binding these dsRNAs via their OST-HTH/LOTUS domains. Indeed, TDRD7 is reported to associate with PIWIL1 (also known as MIWI) protein, which provides the molecular basis for linking the dsRNAs bound by OST-HTH/LOTUS domains to the "effector" PIWI proteins (28, 29).

These remarkable structural and functional similarities between MARF1 and TDRD5/7 proteins led us to propose that MARF1 is a female counterpart to male nuage components, particularly the combination of PIWI proteins with TDRD5/7. The combination of the NYN RNase-like "slicer" domain with OST-HTH/LOTUS domains in MARF1 protein suggests that MARF1 may function as both an adaptor, like TDRD5/7 proteins, to recruit specific RNA targets including those for retrotransposons *Line1* and *Iap*, and an effector, like the PIWI domain in PIWI protein to catalyze the specific cleavages of target RNAs (Fig. 1). Specificity of MARF1 function may be reinforced by the RRM (RNA recognition motif) domain, which is known to bind single-stranded RNAs. With these multiple functional domains, only one key protein, MARF1, could elicit the function carried out by multiple proteins in male germ cell nuage. Nevertheless, the function of MARF1 could well require interacting proteins, and the presence other adaptor molecules in oocytes is certainly possible; however, they apparently do not form visible ribonucleoprotein aggregates similar to male germ cell nuage.

More interestingly, the phylogenetic patterns of OST-HTH/LOTUS domain and NYN domains indicate that they both probably emerged in bacteria (59). With the exception of MARF1, in most eukaryotic OST-HTH/LOTUS domain-containing proteins the OST-HTH/LOTUS domains are fused with different RNA-binding or protein–protein interaction domains. However, almost all of the bacterial versions of OST-HTH/LOTUS domain-containing proteins, similar to MARF1, have one or more OST-HTH/LOTUS domains fused to an N-terminal NYN domain (59). It has been suggested that the OST-HTH/LOTUS domain-containing protein having OST-HTH/LOTUS domains fused with an N-terminal NYN domain is the first version appearing in eukaryotes (59). In this view, MARF1 is probably an ancient protein retaining the role of RNA degradation found in its bacterial cognates. Furthermore, Oskar is also formed by fusion of an OST-HTH/LOTUS domain with a C-terminal "SGNH" hydrolase of bacterial species (Fig. 1) (59, 64). Taken together, these structural considerations suggest that genes for Oskar, TDRD5/7, and MARF1 might have originated from similar ancestors during evolution through gene duplication events and could play conserved roles in germline development.

We assessed similarities in expression of MARF1 and nuage components. In male mice, PIWI proteins and TDRDs are both enriched in germ cells. The expression of PIWIL1 (MIWI) begins in midmeiotic prophase (the pachytene stage) spermatocytes at approximately P14 and persists to the stage of haploid round spermatids (37, 65). PIWIL2 (MILI) is expressed in prospermatogonia of fetal testes beginning at E12.5 and is continuously expressed in germ cells after birth until the stage when haploid round spermatids are formed (12, 36, 65, 66). PIWIL4 (MIWI2) expression also begins in prospermatogonia of fetal testis and persists until shortly after birth (P3) (12). TDRD5 and -7, as most of the other TDRDs including TDRD1, -2, and -7–9, are expressed in both fetal and adult germ cells (5, 31, 39, 67).

Consistent with the expression patterns of PIWIs and TDRDS in male germ cells, MARF1 is highly expressed in fully grown oocytes, but it is barely detectable in the somatic cell compartments of large antral follicles in mouse ovaries (1). Moreover, oocytes express a splice variant of *Marf1*, which is different from the annotated form expressed in somatic cells, and lacks the 3′ 537-bp nucleotides in exon 3. Lack of this part of exon 3 does not change the composition of the major domains in MARF1 protein (1). Although the biological function difference between the oocyte-expressed MARF1 isoform and the somatic cell-expressed MARF1 is not clear, the ovarian function of MARF1 is clearly restricted to oocytes. To further refine the functional window for MARF1 in the control of female fertility, we determined temporal expression of *Marf1* in mouse oocytes and how expression changes during oocyte and preimplantation development. We collected oocytes and preimplantation embryos at different developmental stages and examined the expression of *Marf1* at the levels of both mRNA and protein. As seen in Fig. 2, both *Marf1* mRNA and protein were detected in germ cells as early as the smallest sized oocytes isolated from newborn P0 mouse ovaries. These oocytes are quiescent and have not yet commenced the growth phase. The levels of *Marf1* mRNA and protein increased significantly after oocytes initiated growth, and follicular development reached the primary follicle stage at P6. Thereafter, *Marf1* mRNA and protein remained at the similar levels, both in growing oocytes isolated from early secondary follicles at P12 and in fully grown oocytes isolated from Graafian follicles of equine chorionic gonadotropin (eCG)-stimulated P22 mice. This expression pattern is consistent with that of the *Marf1* β-galactosidase (GAL) reporter, where low X-GAL staining was found in quiescent oocyes of primordial follicles, with extent and intensity of staining increasing in growing and fully grown oocytes (1). Interestingly, this expression pattern of MARF1 in mouse oocytes falls into the window when genome-wide de novo DNA methylation takes place (57). The lower levels of *Marf1* expression in nongrowing oocytes suggest that MARF1 may not play a significant role during early stages of oocyte development.

The steady-state level of *Marf1* mRNA was reduced by approximately half during maturation to the metaphase II (MII) stage, and this level persisted after fertilization and one-cell stage zygote formation (Fig. 2). Thereafter, the levels of *Marf1* mRNA decreased dramatically, by >95%, at two-cell stage embryos and remained constantly low during the following stages of embryo development up to the blastocyst stage. In contrast, levels of MARF1 protein were unchanged during oocyte maturation. This suggests continual translation or stability of MARF1 protein to maintain a constant level, and that MARF1 may play an important role during the processes of oocyte meiotic maturation. At the one-cell stage, even though *Marf1* mRNA levels remained at the same level as in MII oocytes, the protein declined to almost undetectable levels, suggesting posttranslational degradation after fertilization. MARF1 protein remained at barely detectable levels thereafter in two-cell to blastocyst stage embryos, suggesting it does not function during these stages.

As shown previously (1), MARF1 is implicated in retrotransposon suppression in oocytes. Indeed, one key role of the PIWI-piRNA nuage components is to suppress the activation of retrotransposons, particularly *Line1* and/or *Iap*, thereby serving to defend genomic integrity. For example, mutations of *Piwil1*, *Tdrd5*, and *Tdrd7* cause the up-regulation of *Line1* mRNA (25, 39, 40), whereas mutations of *Piwil2* and *Piwil4* result in up-regulation of both *Line1* and *Iap* (13). Similar to these phenotypes, *Marf1*

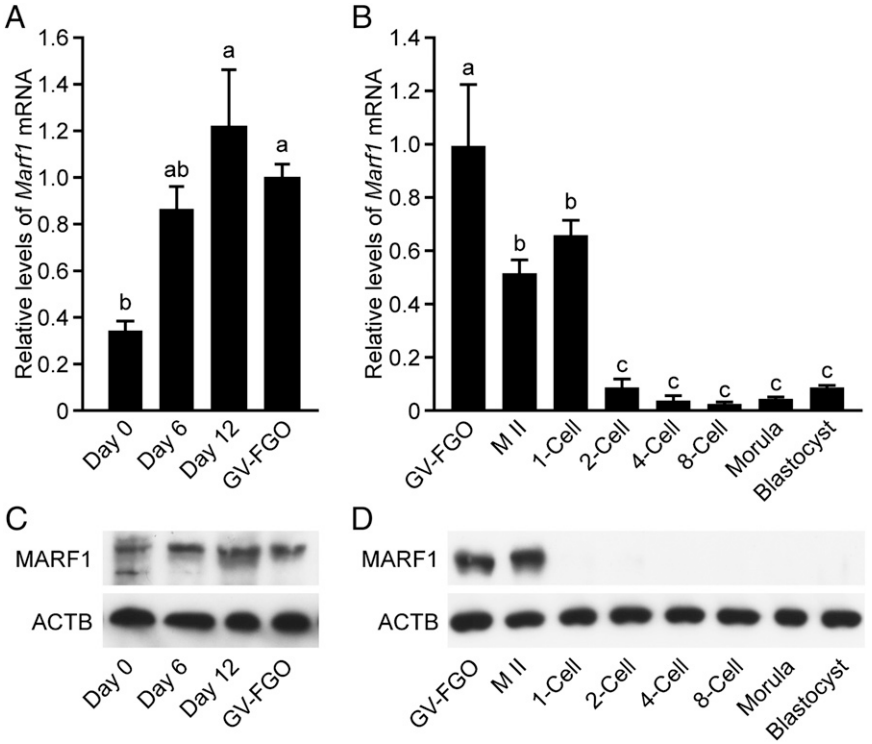

Fig. 2. Expression of *Marf1* in mouse oocytes and preimplantation embryos is developmental stage-dependent. (*A*) Real-time RT-PCR analyses of *Marf1* mRNA levels in developmentally quiescent oocytes isolated from P0 (Day 0) ovaries, growing oocytes isolated from primary follicles of P6 (Day 6) ovaries, growing oocytes isolated from early secondary follicles of P12 (Day 12) ovaries, and GV stage fully grown oocytes (GV-FGO) isolated from large antral follicles of eCG stimulated (46 h) 22-d-old mice. (*B*) Real-time RT-PCR analyses of *Marf1* mRNA levels in GV stage fully grown oocytes, in vivo matured (MII) oocytes, and in vivo developed preimplantation embryos at various stages. (*C* and *D*) Western blot analyses of MARF1 and β-actin (ACTB) protein expression in oocytes at the same stages as in *A* and *B*. In both *A* and *B*, fold changes relative to the GV stage fully grown oocytes group are shown as mean ± SEM ($n = 3$). Bars connected with different letters are significantly different, $P < 0.05$.

mutations cause up-regulation of *Line1* and *Iap* mRNA in fully grown oocytes from large antral follicles (1). However, the temporal onset of this change of *Iap* and *Line1* expression was not known. The presence of MARF1 protein in oocytes of earlier developmental stages could enable the regulation of *Iap* and *Line* mRNA during these early oogenic stages. However, as shown in Fig. 3, no significant up-regulation of *Iap* mRNA was detected in nongrowing oocytes isolated from P0, P6, or P12 *Marf1* mutant mouse ovaries. Nonetheless, *Line 1* mRNA was found to be up-regulated in growing oocytes of P12 *Marf1* mutant ovaries. Therefore, stage-dependent MARF1 regulation of *Iap* and *Line1* retrotransposon expression occurs only after oocyte midgrowth stage, when follicular development advances to the secondary (late preantral) stage. Possibly retrotransposon silencing at earlier developmental stages is by a MARF1-independent mechanism. Notably, DNA methylation of *Iap* and meiotic progression in

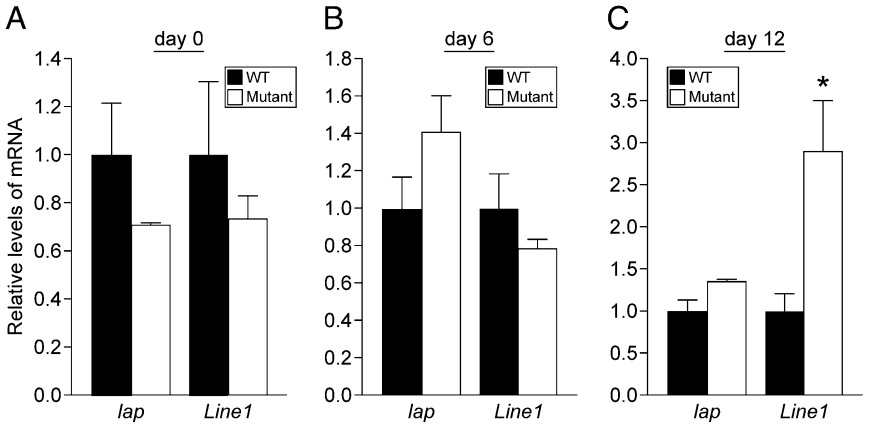

Fig. 3. Up-regulation of retrotransposon mRNAs in *Marf1* mutant oocytes is developmental stage-dependent. Real-time RT-PCR analyses of *Iap* and *Line* mRNA levels in both *Marf1* wild-type and mutant oocytes: (*A*) developmentally quiescent oocytes isolated from P0 newborn mouse ovaries; (*B*) growing oocytes isolated from primary follicles of P6 mouse ovaries; and (*C*) growing oocytes isolated from early secondary follicles of P12 mouse ovaries. Fold changes relative to WT group are shown as mean ± SEM ($n = 3$). Bars connected with different letters are significantly different, $P < 0.05$.

oocytes at earlier developmental stages is regulated by HELLS (formerly known as LSH), a member of the SNF2 family of chromatin remodeling ATPases, which controls accessibility of DNA to de novo DNA methyltransferases DNMT3A and DNMT3B (68). *Hells* knockout oocytes display severe defects in homologous chromosome synapsis, repair of DNA double-stranded breaks, and up-regulation of *Iap* mRNA, which causes meiotic arrest at pachytene stage and subsequent loss of oocytes and failure of ovarian follicle formation (68). This meiotic function of HELLS is apparently not sexually dimorphic, because it also controls early meiotic events in spermatocytes (69); and moreover, the function of HELLS is apparently not germ cell-specific, because HELLS is crucial for normal development, and *Hells* knockout causes early postnatal lethality (70).

The insertion of mobile elements into the host genome after retrotransposon activation causes nuclear DNA double-strand breaks, and indeed we previously observed an increase in the number of DNA double-strand breaks in fully-grown *Marf1* mutant oocytes coincident with up-regulation of *Iap* and *Line 1* mRNA (1). Therefore, we examined the temporal correlation of nuclear DNA double-strand breaks with *Iap* and *Line1* mRNA expression in *Marf1* mutant oocytes. As shown in Fig. S2, oocytes at various stages (leptonema, zygonema, and pachynema) of early meiotic prophase I were found to be present in P0 ovaries, and comparable numbers of positively stained γH2AX foci were found in both wild-type and mutant *Marf1* oocytes at each corresponding meiotic stage, as expected because of the low expression of *Marf1* in wild-type oocytes. This indicates no increase in the number of nuclear DNA double-strand breaks in mutant nongrowing oocytes. Interestingly, unlike male spermatocytes, in which almost all naturally occurring double-strand breaks were already repaired at pachytene stage, a significant number of breaks were still present in both wild-type and mutant pachytene stage oocytes. This hitherto unappreciated sexual dimorphism in meiotic DNA double-strand break repair may help explain observed differences in effects of mutations in this pathway. By the diplotene stage in growing oocytes isolated from both wild-type and mutant P12 ovaries, significantly more γH2AX foci were found in mutant *Marf1* oocytes compared with wild type (Fig. 4), indicating increased DNA double-strand breaks in P12 mutant oocytes.

PIWI proteins and their interacting partners in male germ cell nuage control the activation of retrotransposons at both transcriptional and posttranscriptional levels. Cytosine methylation of the CpG dinucleotides in the promoter region of repetitive elements is a key mechanism for suppressing retrotransposon activation at transcriptional levels in germ cells. In *Tdrd5*-knockout testis, up-regulation of *Line1* mRNA is correlated with demethylation of their promoter elements (39). Similarly, in *Piwil2* and *Piwil4* knockout testis, DNA methylation at *Line1* and *Iap* elements is also significantly reduced (13). These findings prompted us to determine whether the up-regulation of *Line1* and *Iap* mRNAs in *Marf1* fully grown oocytes is accompanied by changes in DNA methylation of their promoter regions. The DNA methylation patterns of *Line1* and *Iap* promoters in *Marf1*wild-type and mutant fully grown oocytes were determined by bisulfite sequencing. As indicated in Fig. 5, comparable numbers of methylated CpGs were identified in the 5′ LTR of *Iap* and 5′ UTRs of two subtypes (type A and type Gf) of *Line1* DNAs, respectively, in both *Marf1* wild-type and mutant oocytes, with no significant difference in the patterns of DNA methylation between wild-type and mutant oocytes at the sites examined. Therefore, up-regulation of *Iap* and *Line 1* mRNAs in *Marf1* mutant oocytes is not caused by suppression of DNA methylation. Although defects in other mechanisms that suppress repetitive elements at transcriptional levels, such as histone modification and heterochromatin formation, could potentially contribute to the up-regulation of *Iap* and *Line* mRNAs in *Marf1* mutant oocytes, a loss of post-transcriptional control of *Iap* and *Line 1* mRNAs seems to be a likely cause. This conclusion is buttressed by our previous observation that, along with up-regulation of *Iap* and *Line1* mRNAs, a significant cohort (377) of transcripts was markedly elevated ≥fourfold in *Marf1* mutant oocytes, whereas only a small number (27) of transcripts was down-regulated to the same extent (1). Furthermore, posttranscriptional regulation by MARF1 protein was also implicated by the observation that, despite dramatic increases in mRNAs of a few representative transcripts from this up-regulated cohort, the levels of their cognate unprocessed heterogeneous nuclear RNA were not changed in mutant oocytes (1). Posttranscriptional regulation of retrotransposon expression also exists in male germ cells. The production of secondary piRNAs through piRNA-guided catalysis of the target retrotransposons by PIWIL2 and PIWIL4 is one major mechanism for post-transcriptional regulation of retrotransposon expression (71). In addition to this piRNA biogenesis-dependent mechanism of silencing retrotransposons, a posttranscriptional mechanism of direct degradation of retrotransposon mRNAs by PIWIL1 occurs in male germ cells. This PIWIL1 "slicer"-dependent mechanism functions without the amplification of piRNAs (25). Interestingly, TDRD7 regulates retrotransposon silencing through a mechanism independent of piRNA biogenesis, one at the level of translational control (40).

The production of piRNA is essential for the PIWI protein-piRNA pathway to function in mouse male germ cells (71). The predicted preference of the OST-HTH/LOTUS domain to bind dsRNAs, particularly those formed by small noncoding RNAs (snRNAs) after hybridizing with their RNA targets, implies that

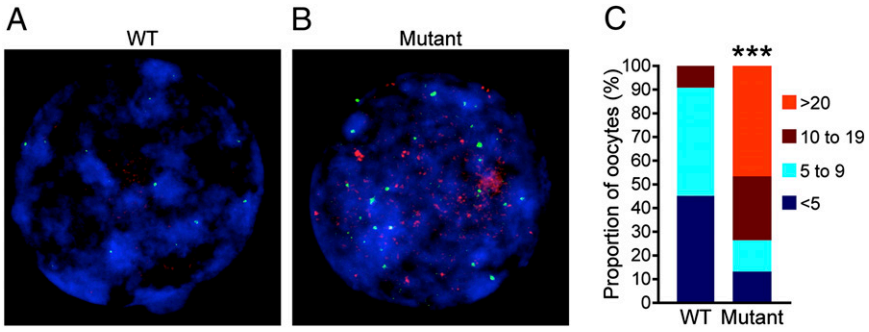

Fig. 4. DNA double-strand breaks are increased in 12-d-old *Marf1* mutant growing oocytes. Confocal microscopy of *Marf1* wild-type (*A*) and mutant (*B*) oocyte chromatin spread and immunolabeled with antibodies to γH2AX (red) and CREST (green) and counterstained with DAPI (blue). (Scale bars, 5 μm.) (*C*) Bar graph showing the proportion of oocytes with various numbers of γH2AX foci in the nucleus. A total of 11 WT and 15 mutant oocytes were scored. ***$P < 0.0005$, χ^2 test.

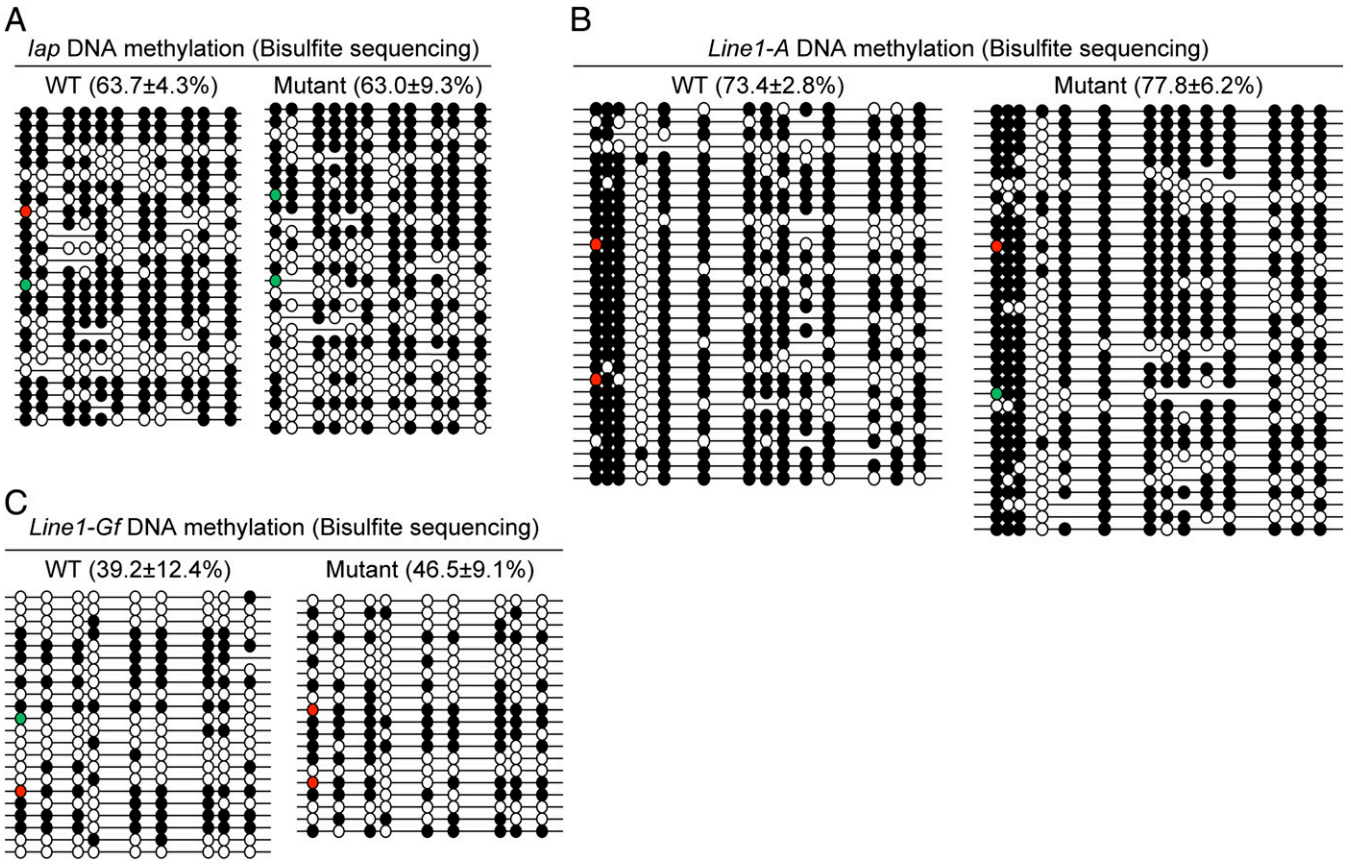

Fig. 5. DNA methylation of retrotransposons is not different in *Marf1* mutant fully grown oocytes compared with wild type. Lollipop diagrams showing the methylation patterns of CpG dinucleotides in the 5′ LTR region of *Iap* (*A*) and 5′ UTRs of *Line1-A* (*B*) and *Line1-Gf* (C), as revealed by bisulfite sequencing, in *Marf1* WT and mutant fully grown oocytes. Three sets of oocyte samples were sequenced, and colored circles indicate the start of sequences for a different set of samples. Circles marked in red indicate methylated CpGs, whereas those marked in green indicate nonmethylated CpGs. The proportion of methylated CpGs is shown as mean ± SEM and is indicated in the parentheses.

the function of MARF1 in mouse oocytes also may require the participation of snRNAs (59). MicroRNAs are abundant in mouse oocytes. However, interruption of miRNA production caused by oocyte-specific knockout of *Dgcr8* does not affect oogenesis and female fertility (72), indicating that miRNAs are not essential for MARF1 function. Endo-siRNAs are also present in mouse oocytes and probably function in the control of oocyte development and repression of retrotransposon expression (2, 3). However, the phenotypes of the oocyte-specific knockout of *Dicer1*, a gene encoding the critical enzyme for miRNA and siRNA production, are different from those of *Marf1* mutants. The *Dicer1*-cKO oocytes can undergo maturation but have severe defects in spindle formation and chromosome alignments (73, 74), and up-regulation of mRNAs for retrotransposons *Mt* and *Sine*, but not *Line 1* and *Iap* (73). This suggests that mouse oocytes use different mechanisms to control different retrotransposable elements. Although a large number of piRNA are detected in mouse oocytes, the role of piRNAs in mouse oocytes remains unknown (2, 3). Whether the functions of MARF1 require the presence of a specific set of piRNAs, or whether MARF1 is actually involved in the production of piRNA in mouse oocytes, awaits investigation.

Concluding Remarks

Sexually dimorphic mechanisms control gametogenic processes in mammals. In males, the RNA "slicer" activity of some PIWI proteins is probably essential for the control of meiosis and silencing of retrotransposons. The function of PIWI proteins requires facilitation by their specific interacting partners—proteins and RNAs tethered together in nuage or germ granules. Tudor domain-containing proteins, such as TDRD5 and TDRD7, play key roles in facilitating the function of PIWIs by acting as scaffolds. In females, no prominent nuage structure is obvious in oocytes, and PIWI proteins and their interacting partners are dispensable for the control of meiosis and retrotransposon silencing. Instead, a female-specific mechanism using MARF1 is used to control these key oogenic processes. Given that the RNase-like NYN domain present in MARF1 protein may resemble the RNA slice activity of PIWI domains in PIWI proteins, and that the OST-HTH/LOTUS that is also present in TDRD5 and TDRD7 may provide specific RNA binding properties, MARF1 alone may be capable of performing regulatory functions similar to those carried out by multiple components in male germ cells. Nevertheless, coordination with other proteins and RNAs may be required for MARF1 function. Identifying these potential partners of MARF1 and resolving their specific interactions will be key to deciphering the molecular mechanisms by which this complex and fascinating protein uniquely orchestrates events essential to oogenesis.

Materials and Methods

Animals. The production and genotyping of *Marf1* wild-type and mutant ($Marf1^{ENU/ENU}$) mice were carried out as described previously (1). Both the $Marf1^{ENU}$ and the C57BL/6JXSJL F1 mice were raised under the standard conditions at the investigators' colonies at The Jackson Laboratory. All mouse procedures and protocols were in accordance with National Institutes of Health guide for animal care and use and were approved by the Animal Care and Use Committee at The Jackson Laboratory.

Chemicals and Reagents. Unless otherwise specified, all chemicals and reagents were purchased from Sigma-Aldrich.

Oocyte and Embryo Isolation. Nongrowing oocytes, growing oocytes from primary and early secondary follicles, GV-stage fully grown oocytes from large antral follicles, and ovulated mature MII oocytes were isolated from newborn mice at P0, P6, and P12, from P22 mice stimulated with equine chorionic gonadotropin (eCG) for 44 h, or from P24 mice first stimulated with eCG for 44 h then human chorionic gonadotropin (hCG) for 14 h, respectively, as described previously (75–77). To obtain preimplantation embryos at various developmental stages, P22 mice were first stimulated with eCG for 44 h and then injected with 5 IU hCG and mated with adult B6SJL F1 male mice. Embryos at one-cell, two-cell, four-cell, eight-cell, morula, and blastocyst stages were then collected from females with visible vagina plugs 18 h, 44 h, 56 h, 68 h, 78 h, and 96 h after receiving hCG injection, respectively.

Real-Time RT-PCR and Western Blot Analyses. These were carried out as described previously (1). To compare the steady-state levels of mRNA in GV-stage fully grown oocytes, MII stage mature oocytes, and preimplanation embryos at various stages of development, the same number (60) of oocytes and preimplantation embryos were used. To normalize potential variation among samples originating from pipetting and RNA isolation processes, rabbit β-globin mRNA was added into each sample at the beginning of RNA extracting process at a concentration of 0.125 pg per oocyte to serve as an external control. In the other real-time RT-PCR experiments, *Rpl19* was used as internal control for normalization of the variation among samples. For Western Blot analysis of MARF1 and ACTB proteins in oocytes at various developmental stages, 60 GV-stage fully grown oocytes, 120 P12 and 480 P6 growing oocytes, and P0 oocytes with the total amount of protein equal to 480 P6 growing oocytes were loaded onto the same gel. For Western Blot analysis of MARF1 and ACTB proteins in oocytes and preimplantation embryos at various developmental stages, the same number (60) of oocytes (GV and MII stages) and preimplantation embryos (one-cell, two-cell, four-cell, eight-cell, morula, and blastocyst stages) were loaded onto the same gel.

Oocyte Spread Preparation and Staining. For preparation of spreads of nongrowing oocytes, ovaries from P0 *Marf1* mutant mice and wild-type littermate controls were collected and rinsed in cold PBS. The ovaries were digested with 0.5 mg/mL collagenase for 30 min in hypotonic extraction buffer (pH 8.2) [15 mM Tris, 50 mM sucrose, 20 mM trisodium citrate, 5 mM EDTA, and a protease inhibitor mixture tablet (Roche)] and then transferred into 100 mM sucrose solution (pH 8.2) and disrupted by pipetting until a single-cell suspension was formed. This ovarian single-cell suspension was subsequently dispensed onto glass slides covered with 1% paraformaldehyde (PFA) containing 0.1% Triton X-100 (pH 9.2) and stayed in a humidified chamber for 3–5 h until the PFA solution was almost dried out. These ovarian cell spreads were washed with 0.4% Photo-Flo (Electron Microscopy Sciences), air dried at room temperature, and stored at −20 °C until being processed for immunofluorescence staining. For preparation of spreads of growing oocytes, ovaries from P12 *Marf1* mutant mice and wild-type littermate controls were collected in cold PBS containing 0.3% BSA, and oocytes were isolated by digesting with 0.1% collagenase as described previously (76). The isolated oocytes were then transferred into 50 μL hypoextraction buffer (15 mM Tris-HCl, 50 mM sucrose, 20 mM citrate, 5 mM EDTA, 0.5 mM DTT, and 0.09 mg/mL PMSF, pH 8.2) and incubated for 30 min at room temperature. After the incubation, 20 μL hypoextraction buffer was replaced with 20 μL 0.1 M sucrose, and the oocytes were incubated for another 30 min. Thereafter, the oocyte spreads were prepared following the same procedure for preparing P0 oocyte spreads as described above. Both the P0 and P12 oocyte spreads were then washed in 10% antibody dilution buffer [3% (wt/vol) BSA, 10% (vol/vol) goat serum, 0.05% Triton X-100] in PBS. The cells were labeled with rabbit anti-phospho-H2AX (γH2AX) (Abcam, catalog no. 07-164) at 1:200, human anti-centromere antibody (Antibodies Incorporated, catalog no. 15-234), rat anti-SYCP3 (see ref. 78 for reference) at 1:1,000. After three washes in PBS, the cells were incubated with secondary antibodies: Alexa Fluor 647 goat anti-rabbit IgG (Invitrogen, catalog no. A21245), Alexa Fluor 594 donkey anti-rat IgG (Invitrogen, catalog no. A21209), Alexa Fluor 488 goat anti-human IgG (Invitrogen, catalog no. A11013), at 1:1,000 at room temperature for 1 h, washed, and mounted onto slides with VecataShield containing DAPI (Vector, catalog no. H-1200) to visualize DNA. The staining was evaluated under a Zeiss Axio Observer Z1 microscope equipped with suitable filters, and images were captured using the attached Zeiss AxioCam camera.

Bisulfite Sequencing. Fifty to 100 *Marf1* wild-type and mutant fully grown oocytes were collected in 10 μL PBS and then subjected to sample lysis and bisulfite conversion using the EpiTect Plus LyseAll Bisulfite Kit (catalog no. 59164, Qiagen) according to the manufacturer's instructions. The resulting DNA were then used for amplification of the selected 5′ LTR region of *Iap* DNA that contains 11 CpGs, and the 5′ UTRs of *Line-Gf* and *Line-A* DNAs that have 9 and 14 CpGs, respectively, using the following primers: *Iap* forward TTGTGTTTTAAGTGGTAAATAAATAATTTG, *Iap* reverse AAAACACCACAAACCAAAATCTTCTAC; *Line1-A* forward TGGATTATAGTGTTTGTTTTAATTTAAT, *Line1-A* reverse TATATTCCACTCACCAAAAATCTT; *Line1-Gf* forward GTTAGAGAATTTGATAGTTTTTGGAATAGG, *Line1-Gf* reverse CCAAAACAAAACCTTTCTCAAACACTATAT. The PCR products were purified using the QIAquick Gel Extraction Kit (catalog no. 28706, Qiagen) and cloned into pCRII-TOPO vector using TOPO TA Cloning Dual Promoter kit (catalog no. K46001, Invitrogen). Positive clones were picked and amplified and plasmid DNA of each clone was purified and sequenced from both ends.

Statistical Analysis. All experiments were performed at least three times, and data are presented as mean ± SEM. In experiments that have only two groups, differences between two groups were analyzed by *t* tests. In experiments having more than two groups, differences between groups were compared by one-way ANOVA followed by Tukey's honestly significant difference test using JMP software (SAS Institute). In the experiment of γH2AX immunostaining, χ^2 was used for analysis of difference between *Marf1* wild-type and mutant groups. Statistical significance was defined as $P < 0.05$.

ACKNOWLEDGMENTS. This study was supported by Grant HD42137 from the Eunice Kennedy Shriver National Institute of Child Health and Human Development.

1. Su YQ, et al. (2012) MARF1 regulates essential oogenic processes in mice. *Science* 335 (6075):1496–1499.
2. Tam OH, et al. (2008) Pseudogene-derived small interfering RNAs regulate gene expression in mouse oocytes. *Nature* 453(7194):534–538.
3. Watanabe T, et al. (2008) Endogenous siRNAs from naturally formed dsRNAs regulate transcripts in mouse oocytes. *Nature* 453(7194):539–543.
4. Juliano C, Wang J, Lin H (2011) Uniting germline and stem cells: The function of Piwi proteins and the piRNA pathway in diverse organisms. *Annu Rev Genet* 45:447–469.
5. Chen C, Nott TJ, Jin J, Pawson T (2011) Deciphering arginine methylation: Tudor tells the tale. *Nat Rev Mol Cell Biol* 12(10):629–642.
6. Castañeda J, Genzor P, Bortvin A (2011) piRNAs, transposon silencing, and germline genome integrity. *Mutat Res* 714(1-2):95–104.
7. Voronina E, Seydoux G, Sassone-Corsi P, Nagamori I (2011) RNA granules in germ cells. *Cold Spring Harb Perspect Biol* 3(12):3.
8. Meikar O, Da Ros M, Liljenbäck H, Toppari J, Kotaja N (2010) Accumulation of piRNAs in the chromatoid bodies purified by a novel isolation protocol. *Exp Cell Res* 316(9): 1567–1575.
9. Huang H, et al. (2011) piRNA-associated germline nuage formation and spermatogenesis require MitoPLD profusogenic mitochondrial-surface lipid signaling. *Dev Cell* 20(3):376–387.
10. Watanabe T, et al. (2011) MITOPLD is a mitochondrial protein essential for nuage formation and piRNA biogenesis in the mouse germline. *Dev Cell* 20(3):364–375.
11. Aravin A, et al. (2006) A novel class of small RNAs bind to MILI protein in mouse testes. *Nature* 442(7099):203–207.
12. Aravin AA, et al. (2008) A piRNA pathway primed by individual transposons is linked to de novo DNA methylation in mice. *Mol Cell* 31(6):785–799.
13. Kuramochi-Miyagawa S, et al. (2008) DNA methylation of retrotransposon genes is regulated by Piwi family members MILI and MIWI2 in murine fetal testes. *Genes Dev* 22(7):908–917.
14. Aravin AA, Sachidanandam R, Girard A, Fejes-Toth K, Hannon GJ (2007) Developmentally regulated piRNA clusters implicate MILI in transposon control. *Science* 316(5825):744–747.
15. Girard A, Sachidanandam R, Hannon GJ, Carmell MA (2006) A germline-specific class of small RNAs binds mammalian Piwi proteins. *Nature* 442(7099):199–202.
16. Grimson A, et al. (2008) Early origins and evolution of microRNAs and Piwi-interacting RNAs in animals. *Nature* 455(7217):1193–1197.
17. Grivna ST, Beyret E, Wang Z, Lin H (2006) A novel class of small RNAs in mouse spermatogenic cells. *Genes Dev* 20(13):1709–1714.
18. Lau NC, et al. (2006) Characterization of the piRNA complex from rat testes. *Science* 313(5785):363–367.
19. Carmell MA, et al. (2007) MIWI2 is essential for spermatogenesis and repression of transposons in the mouse male germline. *Dev Cell* 12(4):503–514.
20. Grivna ST, Pyhtila B, Lin H (2006) MIWI associates with translational machinery and PIWI-interacting RNAs (piRNAs) in regulating spermatogenesis. *Proc Natl Acad Sci USA* 103(36):13415–13420.
21. Cerutti L, Mian N, Bateman A (2000) Domains in gene silencing and cell differentiation proteins: The novel PAZ domain and redefinition of the Piwi domain. *Trends Biochem Sci* 25(10):481–482.

22. Hutvagner G, Simard MJ (2008) Argonaute proteins: Key players in RNA silencing. *Nat Rev Mol Cell Biol* 9(1):22–32.
23. Song JJ, Smith SK, Hannon GJ, Joshua-Tor L (2004) Crystal structure of Argonaute and its implications for RISC slicer activity. *Science* 305(5689):1434–1437.
24. De Fazio S, et al. (2011) The endonuclease activity of Mili fuels piRNA amplification that silences LINE1 elements. *Nature* 480(7376):259–263.
25. Reuter M, et al. (2011) Miwi catalysis is required for piRNA amplification-independent LINE1 transposon silencing. *Nature* 480(7376):264–267.
26. Song JJ, et al. (2003) The crystal structure of the Argonaute2 PAZ domain reveals an RNA binding motif in RNAi effector complexes. *Nat Struct Biol* 10(12):1026–1032.
27. Pek JW, Anand A, Kai T (2012) Tudor domain proteins in development. *Development* 139(13):2255–2266.
28. Chen C, et al. (2009) Mouse Piwi interactome identifies binding mechanism of Tdrkh Tudor domain to arginine methylated Miwi. *Proc Natl Acad Sci USA* 106(48): 20336–20341.
29. Vagin VV, et al. (2009) Proteomic analysis of murine Piwi proteins reveals a role for arginine methylation in specifying interaction with Tudor family members. *Genes Dev* 23(15):1749–1762.
30. Vagin VV, Hannon GJ, Aravin AA (2009) Arginine methylation as a molecular signature of the Piwi small RNA pathway. *Cell Cycle* 8(24):4003–4004.
31. Siomi MC, Mannen T, Siomi H (2010) How does the royal family of Tudor rule the PIWI-interacting RNA pathway? *Genes Dev* 24(7):636–646.
32. Aravin AA, et al. (2009) Cytoplasmic compartmentalization of the fetal piRNA pathway in mice. *PLoS Genet* 5(12):e1000764.
33. Aravin AA, Hannon GJ (2008) Small RNA silencing pathways in germ and stem cells. *Cold Spring Harb Symp Quant Biol* 73:283–290.
34. Cox DN, et al. (1998) A novel class of evolutionarily conserved genes defined by piwi are essential for stem cell self-renewal. *Genes Dev* 12(23):3715–3727.
35. Lin H, Spradling AC (1997) A novel group of pumilio mutations affects the asymmetric division of germline stem cells in the *Drosophila* ovary. *Development* 124(12): 2463–2476.
36. Kuramochi-Miyagawa S, et al. (2004) Mili, a mammalian member of piwi family gene, is essential for spermatogenesis. *Development* 131(4):839–849.
37. Deng W, Lin H (2002) miwi, a murine homolog of piwi, encodes a cytoplasmic protein essential for spermatogenesis. *Dev Cell* 2(6):819–830.
38. Chuma S, et al. (2006) Tdrd1/Mtr-1, a tudor-related gene, is essential for male germ-cell differentiation and nuage/germinal granule formation in mice. *Proc Natl Acad Sci USA* 103(43):15894–15899.
39. Yabuta Y, et al. (2011) TDRD5 is required for retrotransposon silencing, chromatoid body assembly, and spermiogenesis in mice. *J Cell Biol* 192(5):781–795.
40. Tanaka T, et al. (2011) Tudor domain containing 7 (Tdrd7) is essential for dynamic ribonucleoprotein (RNP) remodeling of chromatoid bodies during spermatogenesis. *Proc Natl Acad Sci USA* 108(26):10579–10584.
41. Shoji M, et al. (2009) The TDRD9-MIWI2 complex is essential for piRNA-mediated retrotransposon silencing in the mouse male germline. *Dev Cell* 17(6):775–787.
42. Soper SF, et al. (2008) Mouse maelstrom, a component of nuage, is essential for spermatogenesis and transposon repression in meiosis. *Dev Cell* 15(2):285–297.
43. Tanaka SS, et al. (2000) The mouse homolog of *Drosophila* Vasa is required for the development of male germ cells. *Genes Dev* 14(7):841–853.
44. Ma L, et al. (2009) GASZ is essential for male meiosis and suppression of retrotransposon expression in the male germline. *PLoS Genet* 5(9):e1000635.
45. Frost RJ, et al. (2010) MOV10L1 is necessary for protection of spermatocytes against retrotransposons by Piwi-interacting RNAs. *Proc Natl Acad Sci USA* 107(26): 11847–11852.
46. Zheng K, et al. (2010) Mouse MOV10L1 associates with Piwi proteins and is an essential component of the Piwi-interacting RNA (piRNA) pathway. *Proc Natl Acad Sci USA* 107(26):11841–11846.
47. Handel MA, Eppig JJ (1998) Sexual dimorphism in the regulation of mammalian meiosis. *Curr Top Dev Biol* 37:333–358.
48. Morelli MA, Cohen PE (2005) Not all germ cells are created equal: Aspects of sexual dimorphism in mammalian meiosis. *Reproduction* 130(6):761–781.
49. Yuan L, et al. (2002) Female germ cell aneuploidy and embryo death in mice lacking the meiosis-specific protein SCP3. *Science* 296(5570):1115–1118.
50. Yuan L, et al. (2000) The murine SCP3 gene is required for synaptonemal complex assembly, chromosome synapsis, and male fertility. *Mol Cell* 5(1):73–83.
51. Celeste A, et al. (2002) Genomic instability in mice lacking histone H2AX. *Science* 296 (5569):922–927.
52. Smallwood SA, Kelsey G (2012) De novo DNA methylation: A germ cell perspective. *Trends Genet* 28(1):33–42.
53. Reik W, Dean W, Walter J (2001) Epigenetic reprogramming in mammalian development. *Science* 293(5532):1089–1093.
54. Hajkova P, et al. (2002) Epigenetic reprogramming in mouse primordial germ cells. *Mech Dev* 117(1-2):15–23.
55. Lees-Murdock DJ, De Felici M, Walsh CP (2003) Methylation dynamics of repetitive DNA elements in the mouse germ cell lineage. *Genomics* 82(2):230–237.
56. Li JY, Lees-Murdock DJ, Xu GL, Walsh CP (2004) Timing of establishment of paternal methylation imprints in the mouse. *Genomics* 84(6):952–960.
57. Lucifero D, Mann MR, Bartolomei MS, Trasler JM (2004) Gene-specific timing and epigenetic memory in oocyte imprinting. *Hum Mol Genet* 13(8):839–849.
58. Pepling ME, Wilhelm JE, O'Hara AL, Gephardt GW, Spradling AC (2007) Mouse oocytes within germ cell cysts and primordial follicles contain a Balbiani body. *Proc Natl Acad Sci USA* 104(1):187–192.
59. Anantharaman V, Zhang D, Aravind L (2010) OST-HTH: A novel predicted RNA-binding domain. *Biol Direct* 5:13.
60. Callebaut I, Mornon JP (2010) LOTUS, a new domain associated with small RNA pathways in the germline. *Bioinformatics* 26(9):1140–1144.
61. Anantharaman V, Aravind L (2006) The NYN domains: Novel predicted RNAses with a PIN domain-like fold. *RNA Biol* 3(1):18–27.
62. Lehmann R, Nüsslein-Volhard C (1986) Abdominal segmentation, pole cell formation, and embryonic polarity require the localized activity of oskar, a maternal gene in *Drosophila*. *Cell* 47(1):141–152.
63. Lehmann R, Ephrussi A (1994) Germ plasm formation and germ cell determination in *Drosophila*. *Ciba Found Symp* 182:282–296, discussion 296–300.
64. Lynch JA, et al. (2011) The phylogenetic origin of oskar coincided with the origin of maternally provisioned germ plasm and pole cells at the base of the Holometabola. *PLoS Genet* 7(4):e1002029.
65. Kuramochi-Miyagawa S, et al. (2001) Two mouse piwi-related genes: miwi and mili. *Mech Dev* 108(1-2):121–133.
66. Unhavaithaya Y, et al. (2009) MILI, a PIWI-interacting RNA-binding protein, is required for germ line stem cell self-renewal and appears to positively regulate translation. *J Biol Chem* 284(10):6507–6519.
67. Hosokawa M, et al. (2007) Tudor-related proteins TDRD1/MTR-1, TDRD6 and TDRD7/TRAP: Domain composition, intracellular localization, and function in male germ cells in mice. *Dev Biol* 301(1):38–52.
68. De La Fuente R, et al. (2006) Lsh is required for meiotic chromosome synapsis and retrotransposon silencing in female germ cells. *Nat Cell Biol* 8(12):1448–1454.
69. Zeng W, et al. (2011) Lymphoid-specific helicase (HELLS) is essential for meiotic progression in mouse spermatocytes. *Biol Reprod* 84(6):1235–1241.
70. Geiman TM, et al. (2001) Lsh, a SNF2 family member, is required for normal murine development. *Biochim Biophys Acta* 1526(2):211–220.
71. Bao J, Yan W (2012) Male germline control of transposable elements. *Biol Reprod* 86 (5):162, 1–14.
72. Suh N, et al. (2010) MicroRNA function is globally suppressed in mouse oocytes and early embryos. *Curr Biol* 20(3):271–277.
73. Murchison EP, et al. (2007) Critical roles for Dicer in the female germline. *Genes Dev* 21(6):682–693.
74. Tang F, et al. (2007) Maternal microRNAs are essential for mouse zygotic development. *Genes Dev* 21(6):644–648.
75. Eppig JJ, Wigglesworth K, Hirao Y (2000) Metaphase I arrest and spontaneous parthenogenetic activation of strain LTXBO oocytes: Chimeric reaggregated ovaries establish primary lesion in oocytes. *Dev Biol* 224(1):60–68.
76. Eppig JJ, Schroeder AC (1989) Capacity of mouse oocytes from preantral follicles to undergo embryogenesis and development to live young after growth, maturation, and fertilization in vitro. *Biol Reprod* 41(2):268–276.
77. Eppig JJ (1999) Mouse oocyte maturation, fertilization, and preimplantation development in vitro. *A Comparative Methods Approach to the Study of Oocytes and Embryos*, ed Richter JD (Oxford Univ Press, Oxford), pp 3–9.
78. Eaker S, Pyle A, Cobb J, Handel MA (2001) Evidence for meiotic spindle checkpoint from analysis of spermatocytes from Robertsonian-chromosome heterozygous mice. *J Cell Sci* 114(Pt 16):2953–2965.